

## PRINTED ANTENNA ON FLEXIBLE LOW-COST PET SUBSTRATE FOR UHF APPLICATIONS

Diego Betancourt<sup>1, \*</sup> and Joaquin Castan<sup>2</sup>

<sup>1</sup>Navarra's Research and Technology Multidiciplinar Centre, CEMITEC, Noain 31110, Spain

<sup>2</sup>Miguel de Eguia Technological Centre, CTEL, Estella 31200, Spain

**Abstract**—This paper introduces a flexible antenna, printed on a low-cost Polyethylene Terephthalate (PET) substrate for UHF applications. The RF characteristics of the PET substrate are examined using a microstrip resonator to characterize the substrate's relative permittivity and the loss tangent at UHF band. The PET substrate is used to print an antenna designed to work in the 868 ISM-Band. The printing process described is carried out using a semi-industrial roll-to-roll (R2R) machine with mass production capability. The fabricated dipole antenna was mounted on cylindrical objects made from several materials such as paper and glass, and its RF characteristics were measured and discussed.

### 1. INTRODUCTION

The increasingly use of the UHF RF technologies in the field of Wireless Sensor Networks (WSN) implies the development of medium-range, Medium-bandwidth communications systems with very low power consume and limited cost budget per unit [1]. Particularly attention must be put on the design of the antenna part of such systems in order to maintain the lower cost requirements that suit the economic justification of this kind of projects.

Currently, printed electronics has emerged as a promising technology that has received tremendous interest as a mass production process for low-cost electronic devices (e.g., printed antennas) because it increases manufacturing flexibility and decreases manufacturing costs [2]. At this point, the R2R machine based process becomes

---

*Received 25 January 2013, Accepted 20 March 2013, Scheduled 21 March 2013*

\* Corresponding author: Diego Betancourt (dbetancourt@cemitec.com).

not only the standard for low cost production but it is also more environmentally friendly as it reduces the resulting material waste [3].

Polyethylene Terephthalate (PET) substrate is considered to be one of the best industrial-substrate candidates for UHF and microwave applications since it features the industrial ability to be processed in R2R fashion [4], making it suitable for printed electronics. Nowadays, due to its widespread application scope, in the market could be found several different PET materials, varying in density, coating, thickness, texture, etc.. Because of this, it becomes a must to evaluate the RF characteristics of a PET before to be used as substrate for UHF antennas.

In this paper, the results obtained from the printed dipole antenna on a low cost material are introduced. The material selected for this work is a standard PET. This material is not usually used for high frequency applications but for synthetic fibers; beverage, food and other liquid containers [5]. The PET substrate is characterized using the ring resonator method [6] in the 0 to 6 GHz band. The printing process is a standard industrial method based on flexography carried out by a R2R industrial-type machine, assuring this way a feasible mass production of the printed antennas.

Regular applications of flexible antennas include rough environments, system enclosures or arbitrary 3D forms. In this regard, the fabricated dipole antenna was mounted on cylindrical objects made from several materials such as paper and glass. The RF characteristics of such composites (printed antenna plus support material) were measured.

## 2. RELATED WORK

Printed antennas on PET substrates are a relative novel issue in technical literature. Several work has been done in such respect [4, 5–8, 11]. Most of the work realized in this subject uses substrates suitable to be used in electronic developments as well as in RF designs (e.g., PET film from Krempel, the AKAFLEX PCL) eliminating, this way, prior RF characterization of PET. That is the case of work reported in [7]. When necessary, due to unknown RF characteristics of substrate material to support the printed antenna, the mostly method used is the Ring Resonator method (e.g., for paper characterization in [6]). The work of Jung et al. [4] is an example of the possibilities given by join both the printed electronic field and the industrial production based on a R2R machine.

### 3. PET SUBSTRATE AND R2R MACHINE

The prototypes are designed to be fabricated in the industrial pilot plant. Facilities at the pilot plant include a R2R machine from EDALE reference LAMDA (see Figure 1). This machine allows us to produce semi-industrial series of the printed antenna. The R2R machine is optimum for mass production, reducing the cost of printing on flexible materials. It is equipped with two rollers (unwinder and rewinder, respectively), a printing unit and a curing and sintering zone. A block diagram of the R2R machine is shown in Figure 1.

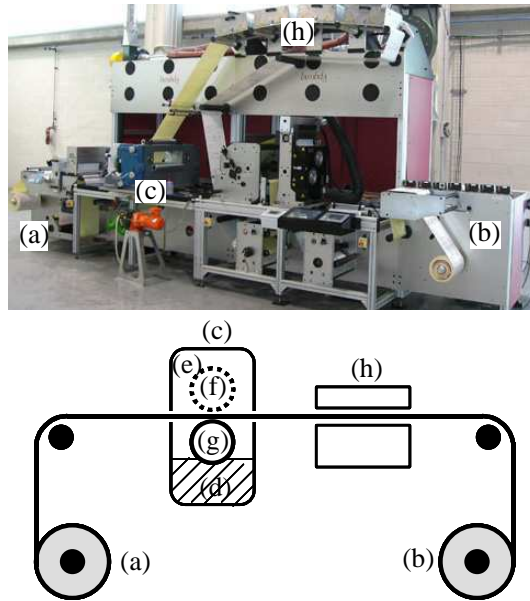


**Figure 1.** Top: R2R printing machine. Bottom: block diagram of R2R machine. (a) Unwinder roller. (b) Rewinder roller. (c) Flexography printer-unit. (d) Ink and chamber. (e) Plate. (f) Print roller. (g) Anilox roller. (h) Belt furnace.

In order to print the RF antenna described in this paper, a flexography printing unit was used. The flexography printing unit consists of a chamber, two rollers (Printer and Anilox) and a plate. The plate is the master-piece with the pattern to be printed in relief. This plate is attached to the Printer. The Anilox is responsible for the transfer of ink from the chamber to the plate. In this stage, a  $10\ \mu\text{m}$  thick silver layer was applied to the PET substrate. The ink used is a silver ink from InkTec (TEC-PR20) composed of silver nano-particles

of 20 to 50 nm in size, with a viscosity of 540cP measured at 20°C.

After this stage, the printed substrate moves along from the printing unit towards the curing and sintering zone, where the ink is dried out and sintered, thus increasing the conductivity of the silver-based ink [1]. The R2R process includes a belt furnace which cures the ink at 130°C, at 8 m/min speed. Lastly, the printed samples are rolled out in the rewinder roller.

In this work we use a thermostabilized PET from MacDermind. PET foils has  $125 \pm 5 \mu\text{m}$  of thickness. Material selected was tested in order to verify PET's shrinkage factor with the temperature-time requirements. According to the antenna requirements, the dimensions can vary a maximum of 2%. The results show material selected is suitable for being used as a substrate since shrinkage measured after 10 min @ 150°C shows an average value of 0.36%.

#### 4. RF CHARACTERIZATION OF PET SUBSTRATE

There are several methods to experimentally determine the RF characteristics of a substrate. The resonator-based methods, including parallel-plate resonators, microstrip ring resonator and cavity resonator are well known. Microstrip ring resonator is the widely-used method in UHF frequency, providing material dielectric information at periodic resonant peaks [6, 10].

The layout of the microstrip ring resonator is shown in Figure 2. The ring resonator produces  $S_{21}$  results with periodic frequency resonances. In this method, relative permittivity  $\epsilon_r$  can be extracted from the location of the resonances of a given radii ring resonator, while loss tangent  $\tan \delta$  is extracted from the quality factor of the resonance peaks along with the theoretical calculations of the conductor losses.

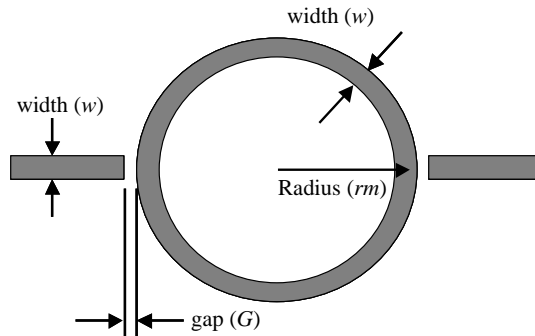


**Figure 2.** Microstrip ring resonator.

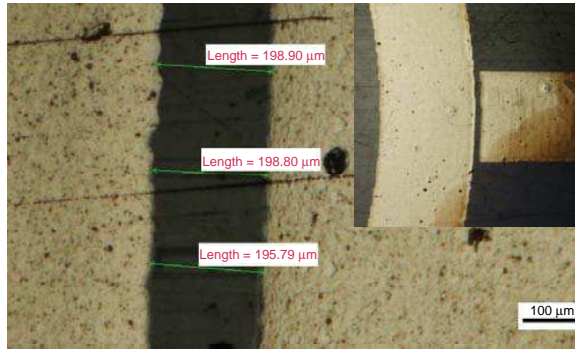


**Figure 3.** Microscope detail of ring resonator’s gap ( $G$ ).

In order to estimate the RF characteristics of PET substrates, two microstrip ring resonators were designed and fabricated. In measurements, a reference plane was set at the edge of the coupling gap to the resonator. Therefore, only the response of the resonating was effectively measured. The full wave electromagnetic solver CST was used to assist the designs. The ring dimensions are: Radii ( $rm$ ), 40 mm; width ( $w$ ), 3 mm; Gap ( $G$ ), 200  $\mu\text{m}$ . A detail of the fabrication of the ring resonator is shown in Figure 3. The microscope view details the Gap ( $G$ ) width confirming its proposed dimensions.

The measurements were performed using an Anritsu MS4623B Vector Network Analyzer (VNA), leading the values listed in Table 1, that features the peaks positions,  $-3$  dB bandwidth and Insertion Loss ( $L_A$ ) at the resonant frequencies, as shown in Figure 4.

The relative permittivity can be extracted from the effective relative permittivity and the dimensions of microstrip by using the formulae proposed in [6, 10].

Values of the relative permittivity extracted at the two resonating modes frequencies for each ring resonator are shown in Table 1. The lowest value obtained was 1.098 and the highest was 1.182 in the range of 0.1–6 GHz. The uncertainty of  $\epsilon_r$  includes errors due to the ring

**Table 1.** Ring resonator resonant modes.

Ring	$N$	$F$ (GHz)	BW <sub>-3 dB</sub> (MHz)	$L_A$ (dBm)	$\epsilon_r$	$\tan\delta$
A	1	2.40	44.9	69.2	1.098	0.039
	2	4.74	134.7	61.9	1.122	0.026
B	1	2.33	104.8	62.6	1.165	0.036
	2	4.62	164.7	47.0	1.182	0.025

resonator dimensions, sample thickness and resonant frequency. A linear average was calculated to estimate the mean value for  $\epsilon_r$  in PET material while its uncertainty interval is estimated using the standard deviation of sample values. For this material, the  $\epsilon_r$  is  $1.142 \pm 0.039$ .

The loss in the rings occurs mainly due to the conductors, lossy dielectrics and radiation. The loss tangent of PET substrate is a function of only the attenuation due to the dielectric characteristics at resonant frequency and is computed using the formulae proposed in [9, 10]. Table 1 shows the  $\tan \delta$  extracted from the two rings at two different frequencies. Loss Tangent values vary from 0.025 to 0.039. The average value obtained for  $\tan \delta$  is  $0.0314 \pm 0.0072$ .

With the aim of verifying the values obtained for  $\epsilon_r$  and  $\tan \delta$  by other methods, a simulation of the results was performed. The average values for  $\epsilon_r$  and  $\tan \delta$  were adopted in the full wave CST simulation. A good agreement in terms of resonant peaks positions between measured and simulated is shown in Figure 4.

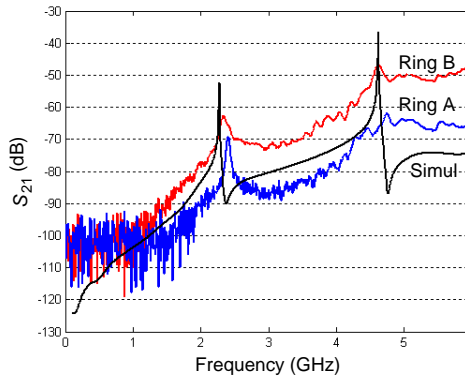


**Figure 4.** Measured and simulated  $S_{21}$  of the two ring resonator configurations. Peak positions and  $-3$  dB bandwidth at two resonant modes ( $N$ ) observed were used to extract the relative permittivity and the loss tangent of PET substrate.

## 5. ANTENNA DESIGN

A dipole antenna, shown in Figure 5, was designed to be printed on PET substrate. Connection of antenna is made via coaxial cable in order to match the antenna to the diverse measurement equipment. For this purpose an SMA-ended pigtail is bounded to antenna substrate. The rigidity of the antenna is assured by adding two clamps to the coax

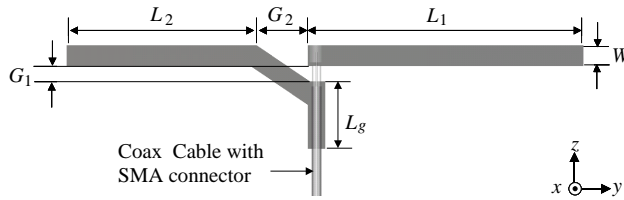


**Figure 5.** Numerical model for printed antenna.

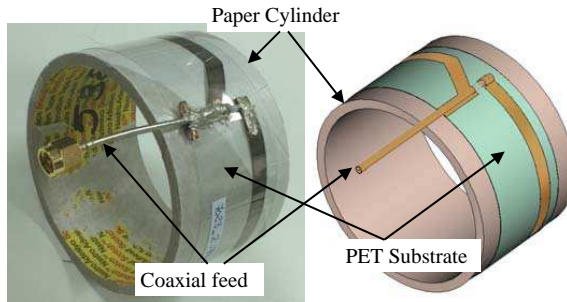


**Figure 6.** Photograph of the antenna bent and bound to a paper cylinder and its numerical model used in simulations.

body and conductor respectively. As is shown in the measurement results, the addition of these clamps does not change the behaviour of the antenna at design frequency at all. The final dipole antenna prototype printed on PET substrate is shown in Figure 6.

The dimensions of the antenna working at UHF frequency, specifically at 869 MHz, are:  $L_1 = 80$  mm;  $L_2 = 55$  mm,  $W = 6$  mm;  $L_g = 19.5$  mm;  $G_1 = 4.5$  mm;  $G_2 = 15$  mm and  $L_{coax} = 70$  mm.

### 5.1. Flexible Printed Antenna

In order to corroborate the good performance of the printed antenna as a flexible antenna, we now introduce the results obtained by bending the printed antenna and attaching it to several materials with different surface characteristics.

Three curved surfaces were selected: a paper cylinder, a glass jar and a PET bottle. First two surfaces are thicker than the printed antenna substrate and they have higher permittivities as well.

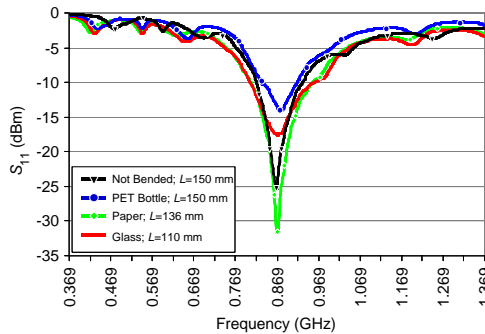
The paper cylinder has the following dimensions: cylinder radii, 25 mm; paper thickness, 5 mm and  $\epsilon_r$ , 2.3. The glass jar used as support for the printed antenna has the following dimensions: radii,

30 mm; thickness, 2 mm and  $\epsilon_r$ , 4,82. Finally, the radii of the PET bottle is 2.9 mm and its thickness 0.8 mm. A picture of the printed antenna mounted over a paper cylinder and its CAD model counterparts are shown in Figure 6.

It is expected the printed antenna's RF characteristics be altered by these new substrates. Particularly, the effect of bending the printed antenna over different surfaces is observed as a frequency shift. This shift in frequency is correspondent with the permittivity of paper and glass respectively.

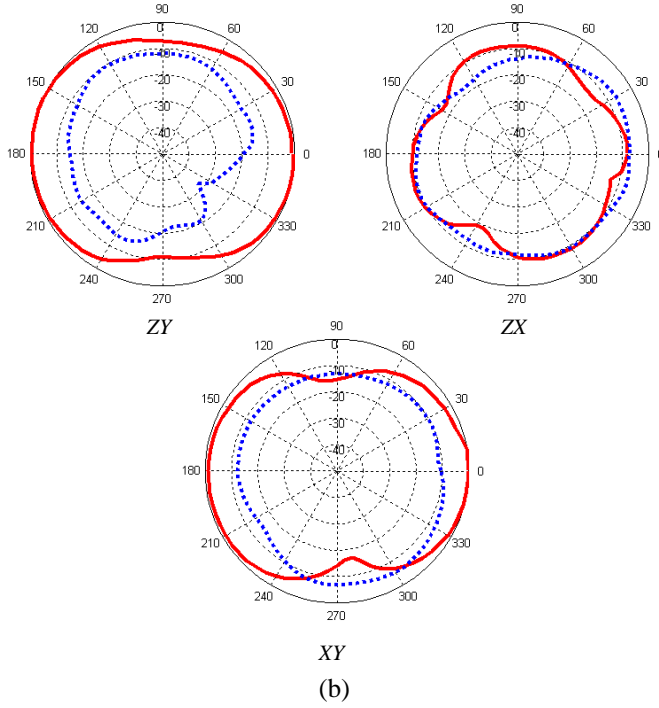
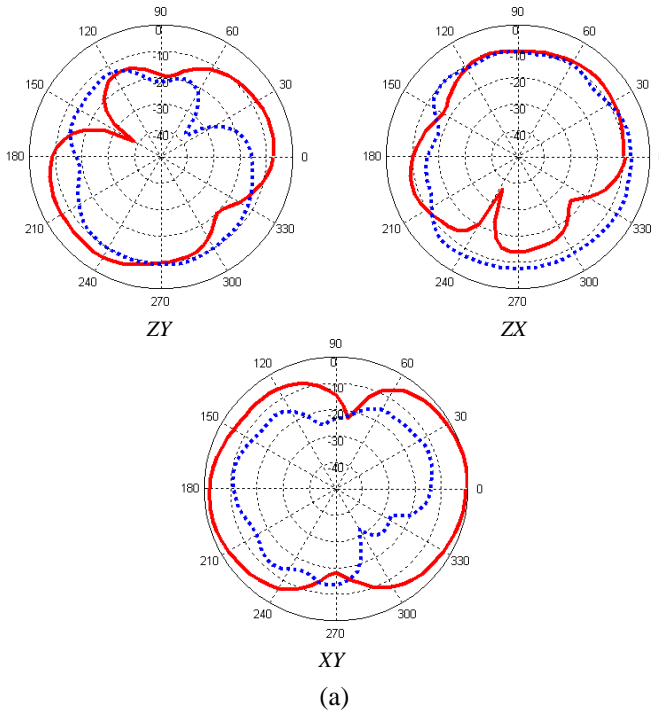
The shift in frequency for antenna composites were corrected to be adapted to 869 MHz, except for PET bottle case, since the antenna composite still matched at desired frequency.

The re-adaptation of antennas' resonant frequency is carried out by symmetrically cutting off the length of radiation arm of printed antenna. The radiation arm of antenna is such composed by strips with length  $L_1$  and  $L_2$  (see Figure 5). Thus, we define  $L$  as the sum of  $L_1 + L_2 + G_2$ . For both not bended antenna and bended over PET bottle antenna length  $L$  is 150 mm; for the antenna bended over paper cylinder  $L$  becomes equal to 136 mm; and for the composite antenna plus glass jar,  $L$  is set to 110 mm. Return loss measurements of printed antennas bent and bonded over the paper cylinder and the glass jar are shown in Figure 7.



**Figure 7.** Return Loss parameters of the printed antennas on PET substrate, bended and attached to a paper cylinder, a PET bottle and a glass jar.

The far field measurements were carried out in an anechoic chamber. The setup proposed for measurement consists of locating the AUT (bended printed antenna) in the  $ZX$ ,  $ZY$  and  $XY$  plane. Each AUT is separated 3 m from the Rx antenna (ETS Lindgren BiConiLog Antenna Model 3142D). By using a VNA (Calibrated at the input ports



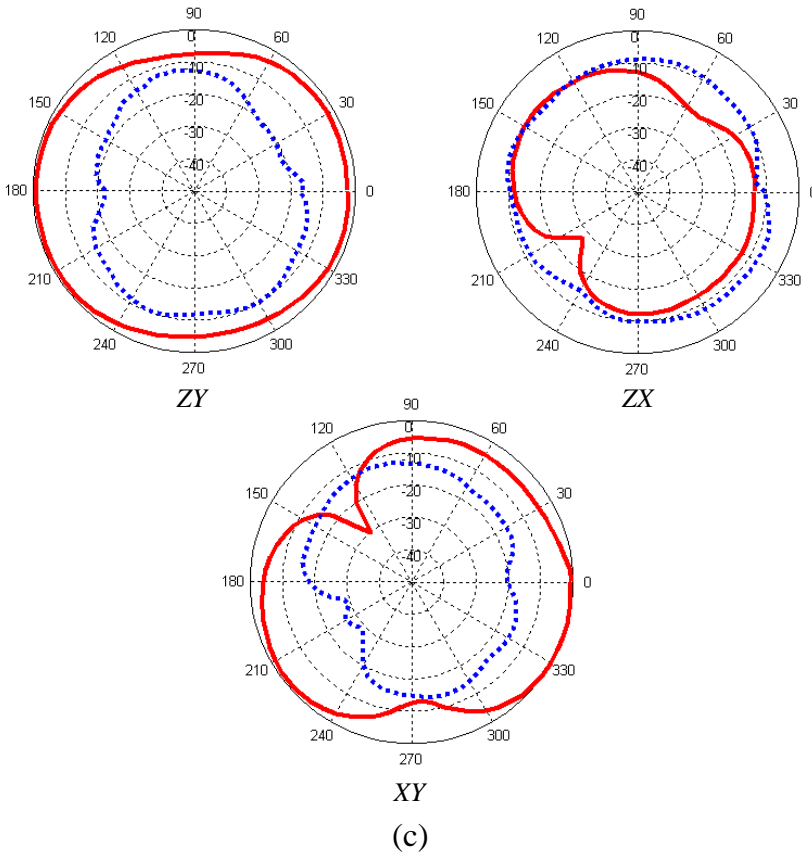


**Figure 8.** Measured Radiation Patterns at Resonant Frequency. Continuous line for Horizontal Polarization and dotted line for Vertical Polarization. (a) Pet bottle. (b) Paper cylinder. (c) Glass jar.

of AUT and Rx antennas),  $S_{21}$  values are captured for Horizontal ( $H$ ) and in Vertical ( $V$ ) configurations. The frequency point selected for measurements corresponds to 869 MHz. Gain of printed antenna is approximately 4.5 dBi and was calculated by using the setup described above.

Figure 8 shows the radiation patterns of printed antennas bent and bonded to several surfaces. Radiation pattern results are normalized. Each composite is measured in  $ZX$ ,  $ZY$  and  $XY$  plane for Vertical and Horizontal Rx antenna polarization. The quasi-omnidirectional pattern of the composite antenna as well as its circular polarization features are observed within far-field results.

## 6. CONCLUSIONS

A printed antenna on low-cost and flexible material was introduced. The substrate used (PET) was studied in order to obtain its RF behavior characteristics at UHF band. An antenna was designed, simulated, fabricated and measured using the PET material as flexible substrate following the procedures of an industrial plant for mass production. The antenna manufactured was measured attached to several materials with bent surfaces. The antenna printed on PET material demonstrated good performance with high bandwidth, good return loss characteristic and adequate radiation patterns.

## REFERENCES

1. Methley, S., *Essentials of Wireless Mesh Networking*, Cambridge, 2009.
2. Forrest, S. R., "The path to ubiquitous and low-cost organic electronic appliances on plastic," *Science*, Vol. 428, No. 6986, 911–918, Apr. 2004.
3. Schwartz, E., "Roll to roll processing for flexible electronics," MSE Thesis, Cornell University, May 2006.
4. Jung, M., J. Kim, J. Noh, N. Lim, C. Lim, G. Lee, J. Kim, H. Kang, K. Jung, A. Leonard, J. Tour, and G. Cho, "All-printed and roll-to-roll-printable 13.56 MHz-operated 1-bit RF tag on plastic foils," *IEEE Trans. on Electron Devices*, Vol. 57, No. 3, 571–580, Mar. 2010.
5. Wang, L., Y. Guo, B. Salam, and C. W. A. Lu, "A flexible modified dipole antenna printed on PET film," *2012 IEEE Asia-Pacific Conference on Antennas and Propagation*, 239–240, Singapore, Aug. 27–29, 2012.
6. Yang, L., A. Rida, R. Vyas, and M. Tentzeris, "RFID tag and RF structures on a paper substrate using inkjet-printing technology," *IEEE Transactions on Microwave Theory and Techniques*, Vol. 55, No. 12, 2894–2901, Dec. 2007.
7. Georgiadis, A., A. Collado, S. Kim, H. Lee, and M. Tentzeris, "UHF solar powered active oscillator antenna on low cost flexible substrate for eireless identification applications," *2012 IEEE MTT-S International Microwave Symposium Digest (MTT)*, 2012.
8. Yoon, H. K., Y. J. Yoon, H. Kim, and C.-H. Lee, "Flexible ultra-wideband polarization diversity antenna with band-notch function," *IET Microwaves, Antennas and Propagation*, Vol. 5, No. 12, 1463–1470, 2011.

9. Gupta, K., R. Garg, I. Bahl, and P. Bhartia, *Microstrip Lines and Slotlines*, 2nd Edition, 108–109, Artech House, Norwood, MA, 1996,
10. Zou, G., H. Gronqvist, P. Starski, and J. Liu, “Characterization of liquid crystal polymer for high frequency system-in-a-package applications”, *IEEE Trans. Advanced Packaging*, Vol. 25, No. 4, 503–508, Nov. 2002.
11. Amin, Y., Q. Chen, H. Tenhunen, and L. R. Zheng, “Performance-optimized quadrate bowtie RFID antennas for cost-effective and eco-friendly industrial applications,” *Progress In Electromagnetics Research*, Vol. 126, 49–64, 2012.